

## Combinatorial Synthesis of Star-Shaped Block Copolymers: Host–Guest Chemistry of Unimolecular Reversed Micelles

Michael A. R. Meier,<sup>†</sup> Jean-François Gohy,<sup>‡</sup> Charles-André Fustin,<sup>‡</sup> and Ulrich S. Schubert<sup>\*†</sup>

Contribution from the Laboratory of Macromolecular Chemistry and Nanoscience, Eindhoven University of Technology and Dutch Polymer Institute (DPI), P.O. Box 513, 5600 MB Eindhoven, The Netherlands, and Unité CMAT and CERMIN, Université catholique de Louvain, Place Pasteur 1, 1348 Louvain-la-Neuve, Belgium

Received March 1, 2004; E-mail: u.s.schubert@tue.nl

**Abstract:** The combination of combinatorial techniques for the synthesis as well as for the screening of novel star-shaped block copolymers consisting of a poly(ethylene glycol) core and a poly(caprolactone) shell leads to a fast evaluation of interesting properties of these materials. The polymers could be synthesized in a fully automated parallel fashion, and the screening of their host–guest properties was accomplished by utilizing a UV/vis plate reader extraction assay. The investigated polymers revealed unimolecular micellar behavior, and their maximum loading capacity could be correlated to their chemical structure. This opens avenues to an improved understanding of the requirements for unimolecular micellar behavior. Furthermore, the accelerated findings clearly point out the advantages of applied combinatorial approaches.

### Introduction

Unimolecular core–shell architectures have gained large attraction during the last years because of their manifold application possibilities, such as drug delivery,<sup>1,2</sup> stimuli responsive release,<sup>3</sup> catalysis<sup>4,5</sup> or phase transfer.<sup>6–8</sup> Compared to micelles formed from amphiphilic molecules, core–shell dendrimers or polymeric unimolecular micelles offer a higher stability in solution since these unimolecular micelles contain covalently fixed branching points. Therefore, no dynamic equilibrium between the individual amphiphile and the self-assembled micellar structure can occur.<sup>9,10</sup> Dendritic nanocarriers for the above-mentioned applications are monodisperse organic chemicals and offer precise control over the chemical structure. However, polymeric systems with core–shell architecture can offer similar properties and do not require a complex multistep synthesis and are therefore accessible in larger scale. Moreover,

upcoming combinatorial techniques in polymer research<sup>11</sup> offer great possibilities for a fast synthesis of new materials as well as the corresponding accelerated property investigation. Utilizing these combinatorial techniques, we report here on the automated and parallel synthesis of star-shaped block copolymers based on a five-arm star-shaped poly(ethylene glycol) (PEG) macroinitiator and the screening of their host–guest properties. This macroinitiator was utilized for the automated parallel controlled ring-opening polymerization of  $\epsilon$ -caprolactone to yield core shell unimolecular micelles with PEG core and poly(caprolactone) (PCL) shell. Previously, it was shown that living and controlled polymerizations could be performed fully automated within a robotic synthesizer.<sup>12,13</sup> Within this contribution, we report on the controlled ring-opening polymerization of  $\epsilon$ -caprolactone<sup>14,15</sup> in an automated synthesizer utilizing a five-arm star-shaped PEG macroinitiator to obtain core–shell-like reversed unimolecular micelles with PEG inner and PCL outer blocks. Thereby, the size of the outer block could be varied to obtain nanocarriers of different molecular weight. Figure 1 depicts the obtained materials, which were subsequently utilized for a host–guest property study. These nanocarriers should be of special interest for biological applications, such as drug delivery, considering the biocompatibility of both blocks.<sup>16,17</sup>

<sup>†</sup> Eindhoven University of Technology and Dutch Polymer Institute.

<sup>‡</sup> Université catholique de Louvain.

- (1) Haag, R. *Angew. Chem., Int. Ed.* **2004**, *43*, 278–282.
- (2) Liu, M.; Kono, K.; Fréchet, J. M. J. *J. Controlled Release* **2000**, *65*, 121–131.
- (3) Krämer, M.; Stambé, J.-F.; Türk, H.; Krause, S.; Komp, A.; Delineau, L.; Prokhorova, S.; Kautz, H.; Haag, R. *Angew. Chem., Int. Ed.* **2002**, *41*, 4252–4256.
- (4) Piotti, M. E.; Rivera, F., Jr.; Bond, R.; Hawker, C. J.; Fréchet, J. M. F. *J. Am. Chem. Soc.* **1999**, *121*, 9471–9472.
- (5) Astruc, D.; Chardac, F. *Chem. Rev.* **2001**, *101*, 2991–3023.
- (6) Goetheer, E. L. V.; Baars, M. W. P. L.; van den Broeke, L. J. P.; Meijer, E. W.; Keurentjes, J. T. F. *Ind. Eng. Chem. Res.* **2000**, *39*, 4634–4640.
- (7) Cooper, A. I.; Londono, J. D.; Wignall, G.; McClain, J. B.; Samulski, E. T.; Lin, J. S.; Dobrynin, A.; Rubinstein, M.; Burke, A. L. C.; Fréchet, J. M. J.; DeSimone, J. M. *Nature* **1997**, *389*, 368–371.
- (8) Ghosh, S. K.; Kawaguchi, S.; Jinbo, Y.; Izumi, Y.; Yamaguchi, K.; Taniguchi, T.; Nagai, K.; Koyoma, K. *Macromolecules* **2003**, *36*, 9162–9169.
- (9) Heise, A.; Hedrick, J. L.; Frank, C. W.; Miller, R. D. *J. Am. Chem. Soc.* **1999**, *121*, 8647–8648.
- (10) Chen, G.; Guan, Z. *J. Am. Chem. Soc.* **2004**, *126*, 2662–2663.

- (11) Meier, M. A. R.; Hoogenboom, R.; Schubert, U. S. *Macromol. Rapid Commun.* **2004**, *25*, 21–33.
- (12) Hoogenboom, R.; Fijten, M. W. M.; Meier, M. A. R.; Schubert, U. S. *Macromol. Rapid Commun.* **2003**, *24*, 92–97.
- (13) Zhang, H.; Fijten, M. W. M.; Reinierkens, R.; Hoogenboom, R.; Schubert, U. S. *Macromol. Rapid Commun.* **2003**, *24*, 81–86.
- (14) Storey, R. F.; Sherman, J. W. *Macromolecules* **2002**, *35*, 1504–1512.
- (15) Kowalski, A.; Duda, A.; Penczek, A. *Macromol. Rapid Commun.* **1998**, *19*, 567–572.
- (16) Nie, T.; Zhao, Y.; Xie, Z.; Wu, C. *Macromolecules* **2003**, *36*, 8825–8829.
- (17) Gan, Z.; Jim, T. F.; Li, M.; Yuer, Z.; Wang, S.; Wu, C. *Macromolecules* **1999**, *32*, 590–594.

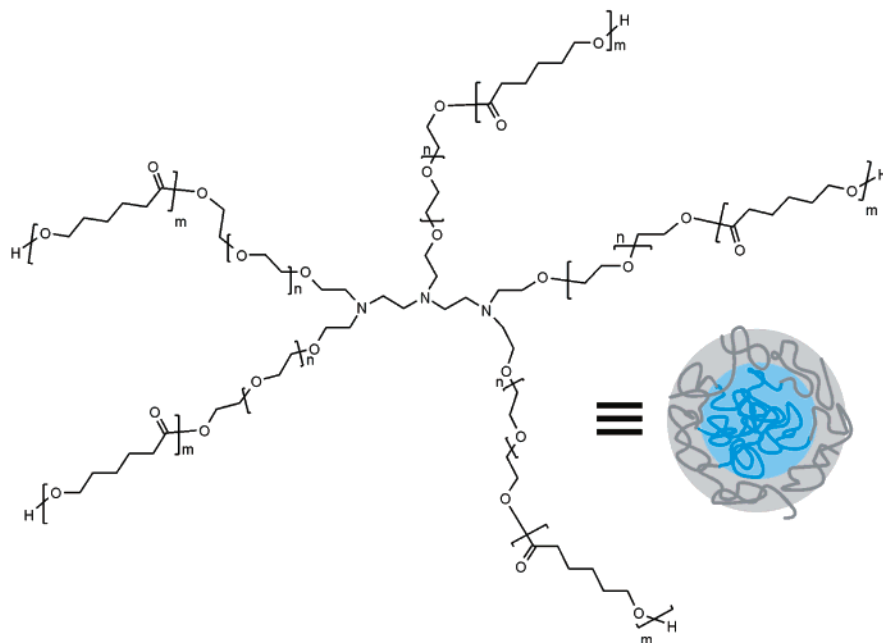


**Figure 1.** Structure and schematic representation of the investigated core–shell nanocarriers consisting of a poly(ethylene glycol) core and a poly(caprolactone) shell.

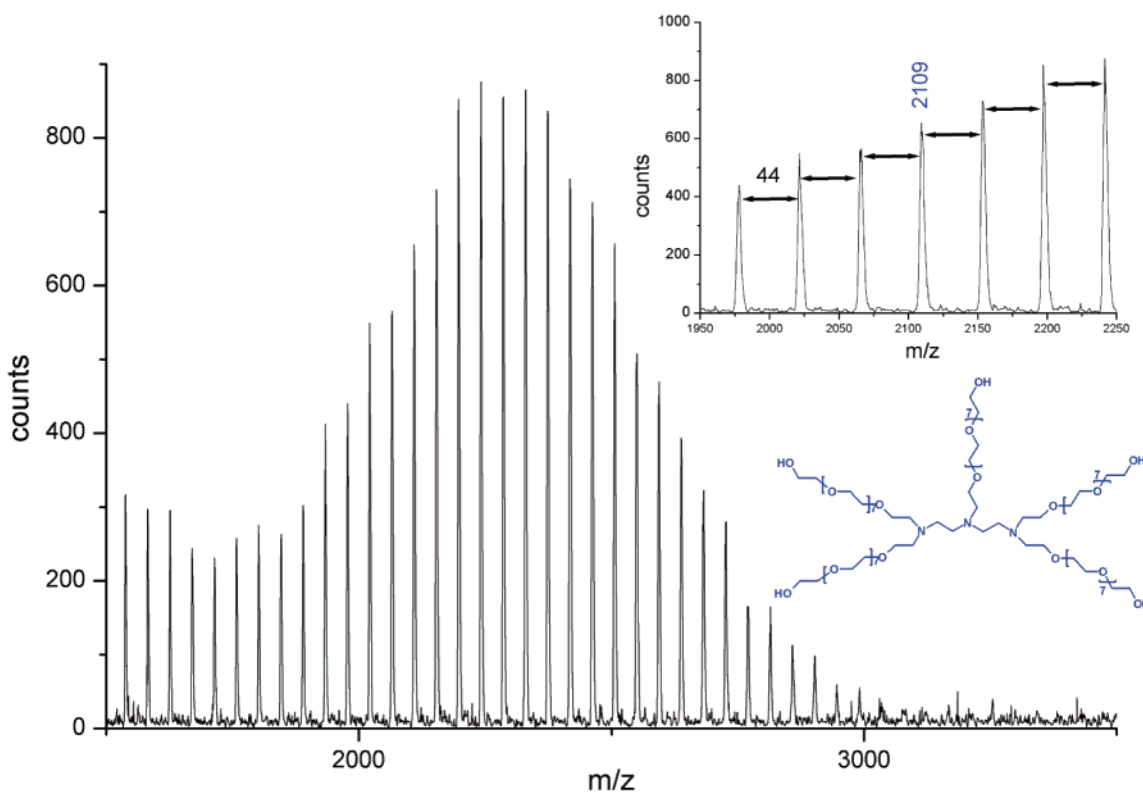


**Figure 2.** MALDI-TOFMS spectrum of the utilized macroinitiator with the corresponding peak assignment.

## Results and Discussion

**Synthesis, Screening, and Characterization.** The synthesis of the investigated star-shaped block copolymers was performed in parallel in a fully automated way utilizing a synthetic robot (for a picture of the ASW200 robot as well as for specifications see, for example, ref 18). However, before actually carrying out the parallel polymerizations the structure of the utilized five-arm star-shaped macroinitiator was confirmed by MALDI-

TOFMS. Figure 2 shows the respective MALDI-TOFMS spectrum with the assigned structure as well as the expected ethylene oxide repeat units of 44 Da. The absolute number-averaged molecular weight ( $M_n$ ) of this MALDI measurement ( $M_n = 2150$ ) was utilized for the calculation of all monomer/initiator (M/I) ratios. Having the structure confirmed, the

(18) Schmatloch, S.; Meier, M. A. R.; Schubert, U. S. *Macromol. Rapid Commun.* **2003**, *24*, 33–46.

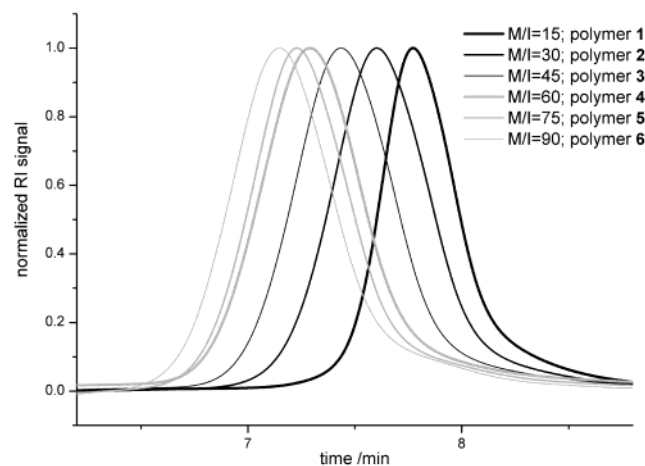


**Figure 3.** GPC traces of the star-shaped block copolymers **1–6** with PEO core and PCL shell.

controlled polymerization of  $\epsilon$ -caprolactone was performed on the ASW2000 automated synthesizer to investigate the controllability as well as reproducibility of the polymerization technique in the robot system. All polymerizations were performed at 130 °C in 2.5 mL of  $\epsilon$ -caprolactone monomer utilizing the five-arm star-shaped PEG macroinitiator and 1/20th of tin catalyst (according to  $-\text{OH}$  functional groups) in 13-mL reactors under a double inert atmosphere. M/I ratios were adjusted and varied to target for different molecular weights. The initiator and the catalyst were transferred as stock solutions (in dichloromethane) to the reactors by the liquid handling system of the robot. After the automated evaporation of the transfer solvent, the monomer was added and the bulk polymerization was performed at 130 °C.

The reproducibility of the applied polymerization technique was investigated by a set of two 4-fold experiments with two different targeted molecular weights. The first set with an M/I ratio of 45 showed only slight variations in the obtained molecular weights and polydispersity indices (PDIs) (both less than 5%) obtained by gel permeation chromatography (GPC). Moreover, the second set of reproducibility experiments with a targeted degree of polymerization (DP) of 60 showed even lower variations of less than 2.5% for the  $M_n$ , weight averaged molecular weight ( $M_w$ ) as well as PDI. Considering the error of GPC measurements of typically 5%, one can conclude that automatically conducted polymerizations were highly reproducible.

Moreover, the control over the parallel polymerization technique can nicely be demonstrated by the fact that it was possible to target for certain degrees of polymerization. Figure 3 depicts gel permeation chromatograms of a series of six star-shaped block copolymers with different molecular weights revealing unimodal molecular weight distributions and moderate PDIs of approximately 1.4 as it can be expected if polymeric materials (PEG initiator:  $M_n = 2150$ ; PDI = 1.1) are utilized as initiators.

The number-averaged molecular weight is increasing with increasing M/I ratio in a linear fashion (see Figure 4) as it can be expected for a controlled polymerization technique. It is known that the hydrodynamic volume of star-shaped polymers is almost independent of their arm number (if all arms bear the same molecular weight) and that therefore the resolution of the separation of these star-shaped polymers by GPC is rather

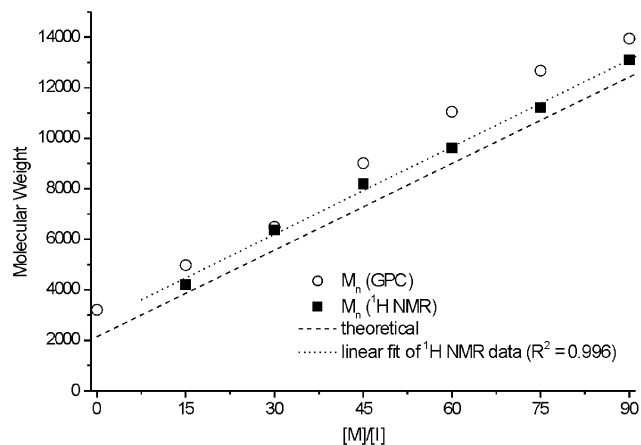


**Figure 4.** Dependence of the number-averaged molecular weight ( $M_n$ ) on the initial M/I ratio for polymers **1–6**.

limited.<sup>19</sup> However, if the number of arms is constant for the investigated system, it is possible to utilize GPC measurements for the comparison of molecular weights of a series of star-shaped polymers and even to obtain linear correlations between targeted and observed molecular weights.<sup>20</sup> Furthermore, one could expect an underestimated molecular weight from GPC measurements because of a smaller hydrodynamic volume of star-shaped macromolecules if compared to their linear analogues.<sup>21,22</sup> However, we obtained higher molecular weights than expected. This effect can be attributed to the nature of the PCL blocks in the polymers. For instance, linear PCL homopolymers consistently show higher molecular weights (factor 1.8–1.9) from GPC measurements on the utilized system if compared to MALDI-TOFMS results. Despite all these difficulties in utilizing GPC to access the molecular weight of star-shaped block copolymers, GPC was able to reveal narrow, monomodal molecular weight distributions for all investigated polymers in an automated and therefore convenient way for combinatorial material research purposes. Before a detailed investigation of polymers **1–6** was performed by  $^1\text{H}$  NMR as well as MALDI-TOFMS, the materials were analyzed by an FT-IR plate reader setup. This allowed the fast and parallel evaluation of copolymer compositions by first normalizing the FT-IR spectra to the C=O stretch vibration at 1735  $\text{cm}^{-1}$  (significant for the PCL block). Subsequently, three signals could be utilized to analyze the composition of the block copolymers **1–6**; they were the C–O stretch vibrations of the PEG monomer units at 1105  $\text{cm}^{-1}$ , the C–H vibrations at 2940 and 2870  $\text{cm}^{-1}$  resulting from both monomer units, and the broad signal at 3500  $\text{cm}^{-1}$  resulting from the R–OH end groups of the polymers.<sup>23</sup> The normalized FT-IR spectra of polymers **1–6** are shown in the Supporting Information of this article and reveal a decrease of all three described signals with increasing molecular weight of the polymers. Therefore, the block copolymer composition changed during the polymerization procedure as expected. Moreover,  $^1\text{H}$  NMR revealed comonomer ratios as they were expected from

- (19) Lee, H. C.; Chang, T.; Harville, S.; Mays, J. W. *Macromolecules* **1998**, *31*, 690–694.  
 (20) Dong, C.-M.; Qui, K.-Y.; Gu, Z.-W.; Feng, X.-D. *Macromolecules* **2001**, *34*, 4691–4696.  
 (21) Lazzari, M.; Kitayama, T.; Jančo, M.; Hatada, K. *Macromolecules* **2001**, *34*, 5734–5736.  
 (22) Cloutet, E.; Fillaut, J.-L.; Astruc, D.; Gnanou, Y. *Macromolecules* **1998**, *31*, 6748–6755.  
 (23) Lang, M.; Wong, R. P.; Chu, C.-C. *J. Polym. Sci., Part A: Polym. Chem.* **2002**, *40*, 1127–1141.

**Table 1.** Monomer/Initiator (M/I) Ratio and  $M_n$  (obtained by  $^1\text{H}$  NMR) of the Investigated Polymers<sup>a</sup>

polymer	1	2	3	4	5	6
$M_n$ (Da)	4200	6370	8200	9630	11 220	13 110
M/I	15	30	45	60	75	90
$D_h^1$ (nm)	$3.1 \pm 0.5$	$3.2 \pm 0.7$	$4.3 \pm 1.0$	$5.1 \pm 0.8$	$5.5 \pm 1.1$	$5.7 \pm 0.9$
$D_h^2$ (nm)	$3.3 \pm 0.7$	$4.2 \pm 0.4$	$5.1 \pm 1.1$	$6.0 \pm 0.9$	$6.8 \pm 0.7$	$8.1 \pm 1.0$

<sup>a</sup> The hydrodynamic diameter ( $D_h$ ) was measured by DLS in THF<sup>1</sup> and in CHCl<sub>3</sub><sup>2</sup> from data extrapolated to zero concentration.

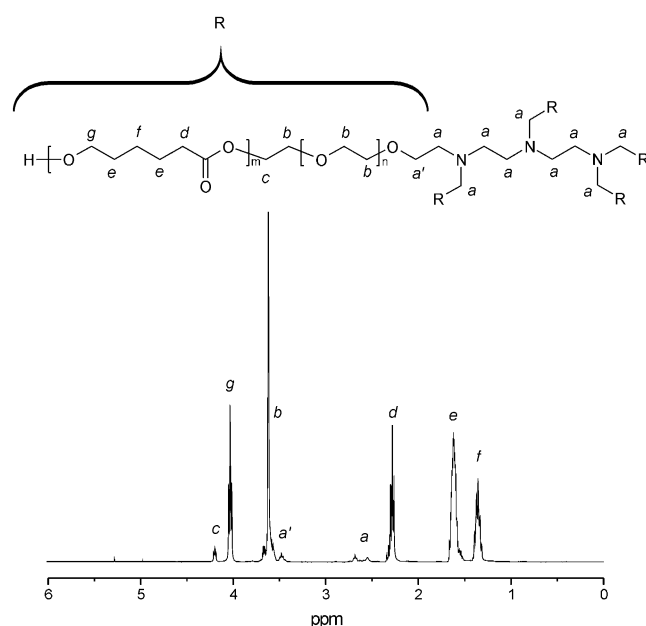


**Figure 5.**  $^1\text{H}$  NMR spectrum of **3** in CDCl<sub>3</sub> with peak assignment. Peak integral values: (a) 18H, (a') 9H, (b) 200H, (c) 10H, (d) 104H, (e) 211H, (f) 107H, (g) 96 H.

initiator and monomer feed ratios for polymers **1–6**. The number-averaged molecular weight as obtained  $^1\text{H}$  NMR analysis of the investigated polymers as well as additional analytical data is summarized in Table 1. Figure 5 shows the  $^1\text{H}$  NMR of **3** in CDCl<sub>3</sub> with assigned signals for one of the five polymer arms. All peak integrals revealed values as expected for the polymeric structure provided in Figure 1. The integral values of signals *c* and *f* were used to calculate  $M_n$  values for polymers **1–6** as they are reported in Table 1. Furthermore,  $^1\text{H}$  NMR revealed a linear correlation between targeted and obtained number-averaged molecular weight ( $M_n$ ), thereby proving the control over the polymerization procedure (Figure 4).

Dynamic light scattering (DLS) data (see Table 1) in THF, a nonselective solvent for the block copolymers, are in agreement with the formation of unimolecular nano objects in which both the core and corona are solvated. The samples were also measured in CHCl<sub>3</sub>, which is, according to the solubility parameters, a better solvent for both the PEO and PCL blocks if compared to THF. This explains why the hydrodynamic volumes ( $D_h$ ) measured in chloroform are systematically higher than those in THF. The angular dependence of the DLS signal revealed that these unimolecular micelles should be spherical in shape.<sup>24</sup>

**Host–Guest Property Screening.** To investigate the host–guest properties of the star-shaped block copolymers **1–6**, the

pH indicator dye methyl orange<sup>25</sup> (acid orange 52, 4-[p(dimethylamino)-phenylazo]benzenesulfonic acid, sodium salt) was chosen for extraction studies in the two-phase chloroform/water system. In this case, the mentioned dye stays in the water phase, whereas upon addition of one of the prepared polymers the dye is extracted into the chloroform phase. This behavior can be explained by encapsulation of the dye in the hydrophilic core of the investigated materials. We were able to evaluate the decreasing concentration of methyl orange in water as a function of added polymer to the two-phase system. Therefore, we measured the overall absorption of the water/chloroform system in transmission mode with a UV/vis plate reader. This allowed a fast and parallel screening of the extraction properties as well as reproducible quantification of the maximum load (ML) of all investigated polymers. For these experiments, 100  $\mu\text{L}$  of a 0.1875 mg/mL solution of methyl orange and 100  $\mu\text{L}$  of polymer containing chloroform solution with different concentrations were pipetted into the wells of the microtiter plate. For each measured microtiter plate, a calibration was also recorded.

Figure 6 shows a filled microtiter plate as utilized for the polymer extraction property screening and some resulting UV/vis spectra. Column one of the microtiter plate was utilized for calibration purposes, whereas all other rows contain different polymers at different concentrations. The concentration of the investigated polymers is increasing from row A to row H. It is clearly visible that, upon addition of a star-shaped block copolymer, the absorption of methyl orange at 504 nm decreases and the absorption maximum of the dye shifts from 504 to 420 nm. This behavior can be explained by an encapsulation and extraction of methyl orange to the organic phase by the polymer. Figure 7 shows an increase of the methyl orange concentration upon addition of polymers **4** and **6**. The concentration of methyl orange was obtained from its decrease in absorption at 504 nm utilizing the simultaneously recorded calibration data. The leveling off of both curves is in agreement with a full extraction of all dye molecules from the water into the chloroform phase. Both findings indicate that these star-shaped block copolymers behave as unimolecular micelles. Moreover, DLS was performed on polymer **6** loaded with MO (five molecules MO per polymer molecule) in chloroform. The  $D_h$  (extrapolated to zero concentration) of  $10.7 \pm 1.3$  nm revealed a swelling of these nano objects upon loading with guest molecules (compare with Table 1). A few percent of larger aggregates were also detected (2%,  $D_h \approx 30$  nm). However, this indicates that the described findings of phase transfer of dye molecules by these star-shaped block copolymers are to large extent a unimolecular micellar effect.

To determine the maximum loading capacity of all investigated polymers, accurately duplicated UV/vis extraction studies in the above-described microtiter plate format were performed. The results are summarized in Table 2 and represent average values of seven parallel measurements for each polymer. The error of these loading values was found to be 0.25 (molecules methyl orange/molecule polymer). These data reveal clearly that all investigated block copolymers show the same extraction capacity of approximately 6.9 dye molecules per molecule of polymer. This can be explained by the unchanged size of the core of the star-shaped block copolymers and indicates that the size of the shell is of minor importance for the loading properties

(24) Berne, B. J.; Pecora, R. J. *Dynamic Light Scattering*; Wiley & Sons: Toronto, 1976.

(25) *Römp Chemie Lexikon*; Falbe, J., Regitz, M., Eds.; Thieme: Stuttgart, 1995; p 2758.



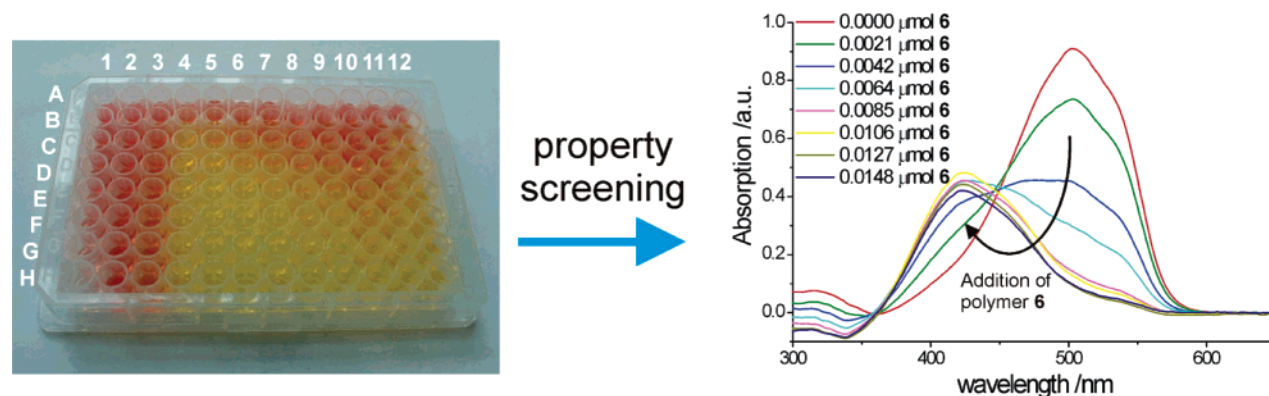


**Figure 6.** Microtiter plate screening of extraction properties of the investigated polymers and a set of corresponding UV/vis spectra. Left: Filled microtiter plate (column 1: calibration; columns 2–12: different polymers; rows A–H: increasing concentration of polymers). Right: resulting UV/vis spectra of one column of the microtiter plate.

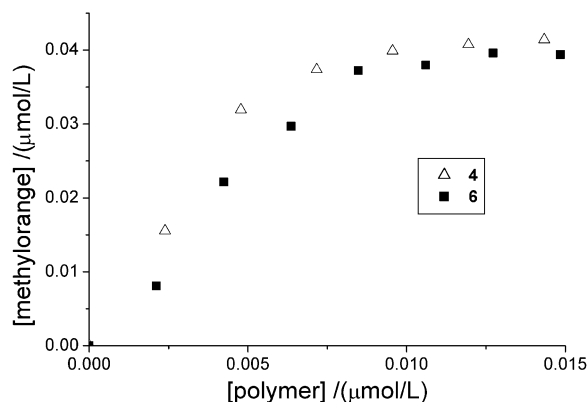


**Figure 7.** Concentration of encapsulated methyl orange as a function of the concentration of polymers 4 and 6.

**Table 2.** Maximum Loading (ML) Values of Polymers 1–6 as Well as Those of the PEG Initiator (INI) in Molecules Methyl Orange per Molecule Polymer

polymer	INI	1	2	3	4	5	6
ML	0.5	7.2	7.2	6.8	7.1	6.9	6.6

of unimolecular micelles. These findings also raise the question if a smaller shell of, for instance, one caprolactone unit or an alkane ether would already be sufficient for a unimolecular micellar behavior. Literature has shown that end group modifications of dendrimers with alkane chains can provide core-shell architectures that can encapsulate dyes<sup>26</sup> or act as catalysts.<sup>4</sup> However, the attachment of PCL chains of different lengths to the branched PEG core allows the adjustment of solubility and maybe even release parameters of these star-shaped block copolymers. Moreover, the utilization of PCL provides biocompatibility and biodegradability of the investigated polymers. Furthermore, the fact that the initiator with the same star-shaped structure has a significantly smaller loading capacity proves that only a core-shell architecture can provide micellar-like behavior. Moreover, it was observed that a linear PEG ( $M_n = 2150$ ; PDI = 1.1) did not show any detectable extraction of methyl

orange in the chloroform/water system. This is in perfect agreement with the comparative study of linear and hyperbranched esterified polyglycerols by Frey et al.<sup>27</sup> and additional proof that a branched polymer structure can freeze in the conformation that is required to obtain unimolecular micellar behavior.

In summary, the utilization of combinatorial techniques for the synthesis as well as for the property screening of new polymeric materials leads to an accelerated discovery of interesting properties of the investigated star-shaped block copolymers. The polymers could be synthesized in a fully automated way, and the screening of their host-guest properties was accomplished by utilizing a new UV/vis plate reader extraction assay. The investigated polymers showed unimolecular micellar behavior. Their loading capacity could be evaluated utilizing the developed extraction assay. Furthermore, a better understanding of the requirements for unimolecular micellar behavior could be established. In conclusion, the investigated materials offer a high potential for applications in catalysis as well as for drug delivery systems, even more if the biocompatibility and/or biodegradability of the utilized materials is taken into account. Moreover, the advantages of star-shaped block copolymers over similar dendrimer systems could recently be demonstrated by the fact that upscaling of the described reaction procedure to multigram scale was possible resulting in a defined polymer in quantitative yield ( $M_n(\text{GPC}) = 10\,550$ ; PDI(GPC) = 1.42; yield = 35 g).

**Acknowledgment.** M.A.R. Meier and U.S. Schubert would like to thank the Dutch Polymer Institute for financial support. C.A. Fustin is Collaborateur Scientifique FNRS.

**Supporting Information Available:** Experimental details as well as additional analytical data (GPC data, DLS details, UV/vis calibration, MALDI-TOFMS of polymer 1, and FT-IR spectra of polymers 1–6). This material is available free of charge via the Internet at <http://pubs.acs.org>.

JA0488481

(26) Baars, M. W. P. L.; Froehling, P. E.; Meijer, E. W. *Chem. Commun.* **1997**, 20, 1959–1960.

(27) Stiriba, S.-E.; Kautz, H.; Frey, H. J. *Am. Chem. Soc.* **2002**, 124, 9698–9699.